Mater. Res. Soc. Symp. Proc. Vol. 876E © 2005 Materials Research Society R7.3.1

Localized and Propagating Surface Plasmon Resonance Sensors: A Study Using Carbohydrate Binding Protein

Chanda Yonzon and Richard P. Van Duyne
Department of Chemistry, Northwestern University
Evanston, IL 60208, U.S.A

ABSTRACT

This work encompasses a comparative analysis of the properties of two optical biosensor platforms: (1) the propagating surface plasmon resonance (SPR) sensor based on a planar, thin film gold surface and (2) the localized surface plasmon resonance (LSPR) sensor based on surface confined Ag nanoparticles fabricated by nanosphere lithography. The binding of Concanavalin A (ConA) to mannose-functionalized self-assembled monolayers (SAMs) is chosen to illustrate the similarities and the differences of these sensors. A comprehensive set of non-specific binding studies demonstrate that the single transduction mechanism is due to the specific binding of ConA to the mannose-functionalized surface. Finally, an elementary (2x1) multiplexed version of a LSPR carbohydrate sensing chip to probe the simultaneous binding of ConA to mannose and galactose-functionalized SAMs is also demonstrated.

INTRODUCTION

The last two decades has seen a tremendous advancement of optical biosensors and their applications in environmental protection,[1,2] biotechnology,[3] medical diagnostics,[4] drug screening,[5] food safety,[2,6] and security.[7] The potential of surface plasmon resonance (SPR) biosensors was realized in early 1980's by Liedberg and coworkers who were able to sense antibodies by observing the change in the critical angle when the antibodies bound selectively to a Au film.[8] Furthermore, in late 1990's, nanoparticle-based localized surface plasmon resonance (LSPR) sensors have been reported to detect biological[9,10] and chemical entities.[11]

Propagating surface plasmons are evanescent electromagnetic waves bounded by flat smooth metal-dielectric interfaces and arise from oscillations of the conduction electrons in the metal.[12] When surface plasmons are confined on either periodic,[13] colloidal,[11] or other nanosystems,[14] localized optical modes are observed. These optical modes lead to highly localized electromagnetic fields outside the particles. Both SPR and LSPR sensors are sensitive to the local refractive index changes that occur when target analyte binds to the metal film or nanoparticles. Surface refractive index sensors have an inherent advantage over optical biosensors that require a chromophoric group or other label to transduce the binding event. Furthermore, they require very little ligand purification due to the specific ligand/receptor binding of these sensors. Also, these sensors provide real-time information on the course of binding and are applicable over a broad range of binding affinities. Additionally, LSPR sensing elements are inherently the size of a single nanoparticle, making the LSPR sensors potentially applicable for *in situ* detection in biological systems. The sensing capability of LSPR sensors can also be tuned by changing the shape, size and material composition of the nanoparticles.[15,16]

This work describes comparative sensor studies conducted on the specific interactions between carbohydrates and proteins using both conventional propagating SPR and the newly developed LSPR sensors. The binding of Concanavalin A (ConA) to mannose-functionalized self-assembled monolayers (SAMs) is chosen to highlight the similarities and differences between the responses of the real-time angle shift SPR and wavelength shift LSPR biosensors. Comprehensive non-specific binding studies are performed to ensure that the signal seen is due to specific binding of ConA to mannose-functionalized surface. Finally, the first multiplexed 2x1 LSPR sensor is also demonstrated.

EXPERIMENTAL DETAILS

Materials. Ag (99.99%) was purchased from D.F. Goldsmith (Evanston, IL) and Au (99.99%) was acquired from Materials Research (Orangeburg, NY). Tungsten vapor deposition boats were purchased from R. D. Mathis (Long Beach, CA). Glass substrates were 18 mm-diameter, no. 2 coverslips from Fisher Scientific (Fairlawn, VA). Pretreatment of glass substrates required H_2SO_4, H_2O_2, and NH_4OH, which were obtained from Fisher Scientific (Fairlawn, VA). Surfactant-free, white carboxyl-substituted polystyrene latex nanospheres with diameters of 390 nm ± 19.5 nm were received as a suspension in water from Duke Scientific (Palo Alto, CA). Ti was purchased from Aldrich (Milwaukee, WI). Phosphate buffered saline (PBS), pH=7.4 was obtained from Sigma (St. Louis, MO). Absolute ethanol was purchased from Pharmco (Brookfield, CT). For all steps of substrate preparation, water purified with cartridges from Millipore (Marlborough, MA) to a resistivity of 18 MΩ was used.

Synthesis. The compounds 11-mercaptoundecyl tri(ethyelene glycol) disulfide (EG3), malemide terminated disulfide, mannose thiol, and galactose thiol were synthesized as described in the literature.[17]

Nanosphere lithography (NSL). Glass substrates were pretreated in two steps (1) piranha etch, 1:3 30% H_2O_2:H_2SO_4 at 80ºC for half an hour to clean the substrate, and (2) base treatment, 5:1:1 H_2O:NH_4OH:30% H_2O_2 with sonication for 1 hr, which rendered the surface hydrophilic. Both piranha etch and base treatment were done in the hood with appropriate safety goggles and lab coats. Approximately 2 µL of undiluted nanosphere solution (10% solid) were drop-coated on the pretreated glass. The nanospheres were allowed to dry in ambient conditions to form a 2D hexagonally close packed array. Ag was thermally deposited and the sphere mask was removed by sonication in absolute ethanol for 3 min.

SPR and LSPR sensor preparation. For the SPR sensor, Au (50 nm) was evaporated on glass coverslips with a thin Ti underlayer (10 nm) for adhesion of Au. On the other hand for the LSPR sensors, NSL created Ag nanoparticle arrays were used. The SAM was prepared by immersing the coverslips in an ethanolic solution containing 450 µL tri(ethylene glycol) disulfide (EG3), (1 mM), and 50 µL maleimide-terminated disulfide, (1 mM). After twelve hours, the coverslips were rinsed with ethanol and dried under a stream of nitrogen. The substrates presenting maleimide-functional groups were

immersed in methanolic solutions of 5 mM mannose thiol**,** for 40 min. The mannose thiol covalently binds to malemide, providing ~5% sugar-immobilized surfaces, based on the fraction of starting thiols and efficiency of the malemide reaction.[18] The mannose-functionalized sensors were then exposed to ConA for 20 min.

SPR Spectroscopy. A BIACore 1000 (Neuchâtel, Switzerland) was used for all propagating SPR measurements reported here. The mannose-functionalized substrate was incorporated into BIAcore cassettes by gluing the chip into the cassettes using a Devcon two-part epoxy (Danvers, MA). PBS, pH 7.4, was used as the running buffer and measurements were reported as changes in resonance angle ($\Delta\theta$), where 1° = 10000 RU.

LSPR spectroscopy. LSPR extinction measurements were taken using an Ocean Optics (Dunedin, FL) SD2000 fiber optically-coupled spectrometer. All spectra in this study were from macroscopic measurements obtained in transmission mode using unpolarized white light with a probe diameter of ~2 mm. A home built flow cell was used to control the surrounding environment of the Ag nanoparticles and to introduce the analytes.

RESULTS AND DISCUSSION

Comparison of real-time binding studies. Van Duyne and coworkers have previously demonstrated detection of various biomolecules using LSPR sensors.[9,19] In this study, the real-time response of the flat surface SPR sensor (Figure 1A) and the LSPR Ag nanosensor (Figure 1B), the SPR response ($\Delta\theta$) and LSPR $\Delta\lambda_{max}$ response to the ConA binding on the mannose-functionalized surface was investigated. First, SPR $\Delta\theta$ response of the mannose-functionalized Au surface in a running buffer environment was recorded, followed by 19 μM ConA injection. Then, the sensor was flushed with buffer for removal of non-specifically bound ConA and a partial dissociation of ConA bound as the 1:1 mannose complex. Figure 1A illustrates the real-time monitoring of ConA by the SPR $\Delta\theta$ shift. Similarly, the real-time LSPR response of ConA binding to

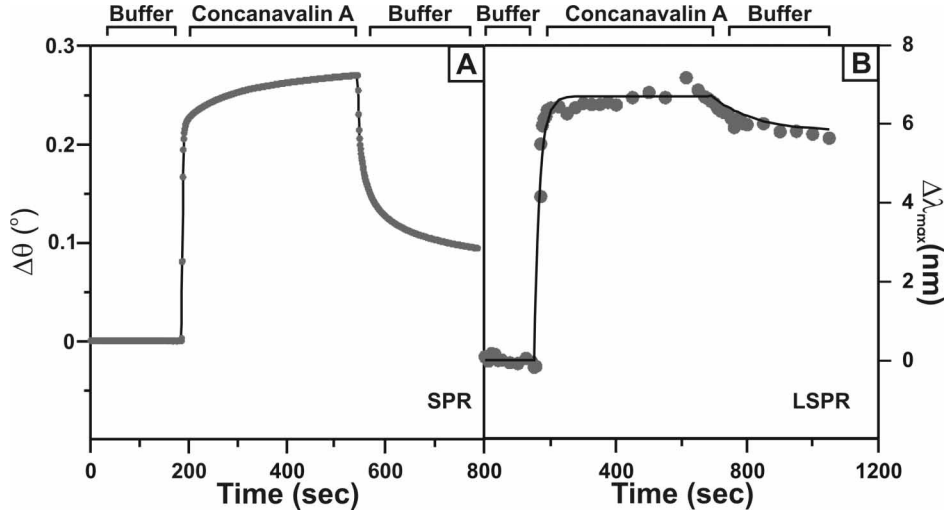

Figure 1: Real-time response of sugar-functionalized sensor as ConA was injected in the cell following buffer injection.

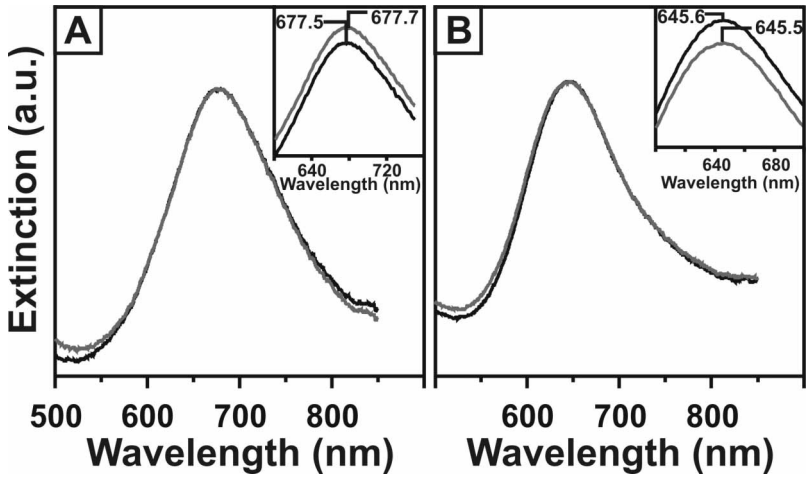

Figure 2. Non-specific binding study on mannose functionalized Ag nanosensor with two different proteins. All insets magnify the extinction spectra and the λ_{max} are denoted.

the mannose-functionalized Ag nanonsensor was also probed (Figure 1B).

Both the SPR and LSPR sensor showed a rapid response when ConA was exposed to the surface during the association phase, which indicates strong 1:1 mannose/ConA binding on the surface[20] followed by weak non-specific binding. However during the dissociation phase, the response of the SPR sensor decreased by 60% whereas the response of the LSPR sensor decreased only by 14%. Our working hypothesis to explain this difference is the long range decay length of the SPR sensor electromagnetic field ($l_d \approx 200$ nm),[21] compared to that of the LSPR sensor ($l_d \approx$ 5-6 nm).[19] The dissociation response seen in the SPR sensor is caused by removal of non-specifically bound ConA, partial dissociation of 1:1 bound ConA with mannose, and change in bulk refractive index from ConA/buffer to only buffer.[17] However, due to shorter decay length of the electromagnetic field of the LSPR sensor, the dissociation response seen can be attributed to only removal of non-specifically bound ConA and partial dissociation of bound ConA.

Non-specific binding studies. To verify that the SPR and LSPR responses seen when ConA binds to the mannose functionalized surface is due solely to specific binding between the ligand and the receptor, two non-specific binding studies listed below were performed.

1) Erythrina Crystagalli (Ery) interacting with the mannose functionalized sensor. Ery is a dimer plant lectin with molecular weight of 56 kDa that specifically binds to galactose.[22] The Ag nanosensors were exposed to Ery to demonstrate that the mannose-functionalized Ag nanosensors do not have an affinity toward lectins other than mannose binding lectins. The Ag nanosensors functionalized with mannose SAMs had a LSPR λ_{max} of 677.5 nm (Figure 2A). Incubation of the sensor in 26 μM Ery resulted in a LSPR λ_{max} of 677.7 nm. The 0.2 nm shift corresponds to the instrumental noise wavelength shift in the baseline, illustrating that lectins not specific to mannose do not bind to the mannose-functionalized sensor surface.

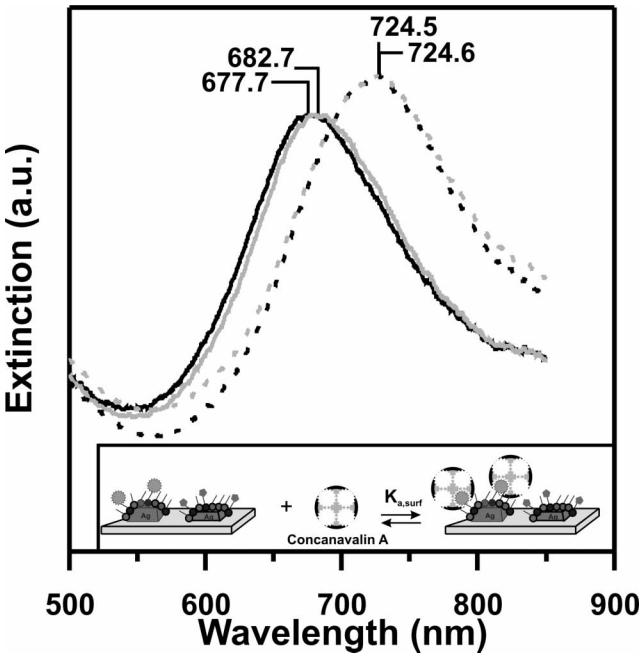

Figure 3. LSPR spectra illustrating multiplexing Ag nanosensor carbochip. Inset shows the schematic of selective ConA binding to the mannose-functinalized portion of the chip.

2) BSA interacting with the mannose-functionalized sensor. The Ag nanosensors were exposed to a BSA solution to demonstrate that they neither have an affinity toward other lectins, nor interact with other proteins. The Ag nanoparticles were functionalized with mannose thiols giving a LSPR λ_{max} of 645.6 nm (Figure 2B). Incubation of the sensor in 29 μM BSA resulted in a LSPR λ_{max} of 645.5 nm, which too is equal to the instrumental noise.

Fabrication of a LSPR carbohydrate sensing chip. A (2x1) LSPR carbohydrate sensing chip sensor consists of a glass substrate with nanoparticle arrays of two different heights (viz. 35 nm and 75 nm). The 35 nm nanoparticle arrays were functionalized with galactose resulting into a LSPR λ_{max} of 724.5. Similarly, 75 nm nanoparticle arrays were functionalized with mannose resulting into a LSPR λ_{max} of 677.7 nm. To prevent the mixing of the sugar thiol solutions, the nanoparticle array elements were separated by a poly(dimethyl siloxane) seperator and was removed before exposing the surface to ConA. The galactose and mannose-functionalized carbohydrate sensing chip was exposed to 19 μM ConA and rinsed with PBS buffer resulting in a LSPR λ_{max} of 724.6 nm and 682.7 nm (Figure 3).

When ConA binds to the mannose-functionalized surface, a 5 nm shift is seen, and when the ConA binds to the galactose-functionalized surface, a 0.1 nm shift is observed indicating that no binding occurs. The decrease in the LSPR shift seen when ConA binds to the mannose-functionalized Ag nanosensor with out-of-plane height of 75 nm is attributed to the lower refractive index sensitivity of taller nanoparticles.[16,23]

CONCLUSION

In this work, we have compared the responses of a SPR sensor with a LSPR sensor using the binding of ConA to a mannose-functionalized SAM surface. Real-time angle shift SPR and wavelength shift LSPR measurements exhibited comparable magnitude saturation coverage responses during the association phase when ConA specifically bound to mannose ligand. However during the dissociation phase, the signal loss for SPR sensor was 5 times greater than that of the LSPR sensor. In addition, to verify that the response seen on the LSPR sensor was due to the specific binding of ConA to the mannose-functionalized Ag nanosensor, several non-specific binding studies were

performed. Finally, this work demonstrates the first multiplexed version of a LSPR carbohydrate sensing chip to study the affinity of ConA on the mannose and galactose-functionalized surface.

ACKNOWLEDGEMENTS

The authors gratefully acknowledge Ms. Liza Babayan and Dr. Douglas A. Stuart for their technical assistance and helpful discussions. This project was supported by the Nanoscale Science and Engineering Initiative of the National Science Foundation under NSF Award EEC-0118025.

REFERENCES:

(1) Ji, J.; Schanzle, J. A.; Tabacco, M. B. *Anal. Chem.* **2004**, *76*, 1411-1418.
(2) Ligler, F. S.; Taitt, C. R.; Shriver-Lake, L. C.; Sapsford, K. E.; Shubin, Y.; Golden, J. P. *Anal. Bioanal. Chem.* **2003**, *377*, 469-477.
(3) Kohls, O.; Scheper, T. *Sens. Actuators B* **2000**, *70*, 121-130.
(4) Yonzon, C. R.; Haynes, C. L.; Zhang, X.; Walsh, J. T.; Van Duyne, R. P. *Anal. Chem.* **2004**, *76*, 78-85.
(5) Ho, H.; Leclerc, M. *J. Am. Chem. Soc.* **2004**, *126*, 1384-1387.
(6) Wiskur, S. L.; Anslyn, E. V. *J. Am. Chem. Soc.* **2001**, *123*, 10109-10110.
(7) Bauer, G.; Hassmann, J.; Walter, H.; Haglmueller, J.; Mayer, C.; Schalkhammer, T. *Nanotech.* **2003**, 1289-1311.
(8) Liedberg, B.; Nylander, C.; Lundstorm, I. *Sens. Actuators B* **1983**, *4*, 229-304.
(9) Riboh, J. C.; Haes, A. J.; McFarland, A. D.; Yonzon, C. R.; Van Duyne, R. P. *J. Phys. Chem. B* **2003**, *107*, 1772-1780.
(10) Yonzon, C. R.; Zhang, X.; Van Duyne, R. P. *Proc. SPIE* **2003**, *5224*, 78-85.
(11) McFarland, A. D.; Van Duyne, R. P. *Nano Lett.* **2003**, *3*, 1057-1062.
(12) Reather, H. *Surface Polaritons on Smooth and Rough Surfaces and on Gratings*; Springer-Verlag: Berlin, 1988.
(13) Garcia-Vidal, F. J.; Pendry, J. B. *Phys. Rev. Lett.* **1996**, *77*, 1163-1666.
(14) Jensen, T. R.; Schatz, G. C.; Van Duyne, R. P. *J. Phys. Chem. B* **1999**, *103*, 2394-2401.
(15) Haynes, C. L.; Van Duyne, R. P. *J. Phys. Chem. B* **2001**, *105*, 5599-5611.
(16) Haes, A. J.; Zou, S.; Schatz, G. C.; Van Duyne, R. P. *J. Phys. Chem. B* **2004**, *108*, 109-116.
(17) Houseman, B. T.; Gawalt, E. S.; Mrksich, M. *Langmuir* **2003**, *19*, 1522-1531.
(18) Folkers, J. P.; Laibinis, P. E.; Whitesides, G. M. *J.Phys.Chem* **1994**, *98*, 563-571.
(19) Haes, A. J.; Van Duyne, R. P. *J. Am. Chem. Soc.* **2002**, *124*, 10596-10604.
(20) Smith, E. A.; Thomas, W. D.; Kiessling, L. L.; Corn, R. M. *J. Am. Chem. Soc.* **2003**, *125*, 6140-6148.
(21) Jung, L. S.; Campbell, C. T.; Chinowsky, T. M.; Mar, M. N.; Yee, S. S. *Langmuir* **1998**, *14*, 5636-5648.
(22) Gupta, D.; Cho, M.; Cummings, R. D.; Brewer, C. F. *Biochem.* **1996**, *35*, 15236 - 15243.
(23) Jensen, T. R.; Malinsky, M. D.; Haynes, C. L.; Van Duyne, R. P. *J. Phys. Chem. B* **2000**, *104*, 10549-10556.